

## Analysis of delay compensation in real-time dynamic hybrid testing with large integration time-step

Fei Zhu, Jin-Ting Wang\*, Feng Jin, Yao Gui and Meng-Xia Zhou

*State Key Laboratory of Hydrosience and Engineering, Tsinghua University, Beijing, China*

*(Received April 10, 2014, Revised August 17, 2014, Accepted August 20, 2014)*

**Abstract.** With the sub-stepping technique, the numerical analysis in real-time dynamic hybrid testing is split into the response analysis and signal generation tasks. Two target computers that operate in real-time may be assigned to implement these two tasks, respectively, for fully extending the simulation scale of the numerical substructure. In this case, the integration time-step of solving the dynamic response of the numerical substructure can be dozens of times bigger than the sampling time-step of the controller. The time delay between the real and desired feedback forces becomes more striking, which challenges the well-developed delay compensation methods in real-time dynamic hybrid testing. This paper focuses on displacement prediction and force correction for delay compensation in the real-time dynamic hybrid testing with a large integration time-step. A new displacement prediction scheme is proposed based on recently-developed explicit integration algorithms and compared with several commonly-used prediction procedures. The evaluation of its prediction accuracy is carried out theoretically, numerically and experimentally. Results indicate that the accuracy and effectiveness of the proposed prediction method are of significance.

**Keywords:** real-time dynamic hybrid testing; delay compensation; sub-stepping technique; large integration time-step; displacement prediction; explicit integration algorithm

### 1. Introduction

Real-time dynamic hybrid testing (RTDHT) is an effective method to analyze dynamic responses of complex structures that are excited by earthquake loads. It divides the entire structure system into numerical and physical substructures, which are simulated in computers and experimented by loading equipments, respectively. The term “real-time” is a double-edged sword for the RTDHT. On one hand, it ensures the realistic loading rate of the physical substructure to enable the simulation of rate-dependent behavior of structures; on the other hand, it imposes quite high performance requirements for loading equipments, numerical integration algorithms, and data transmission, which limits the simulation scale of structures and restricts the rapid promotion of the RTDHT to engineering application.

To simulate complex and large-scale numerical substructures in real-time, the enlargement of the integration time-step is an effective strategy. However, the sampling time-step of the controller

---

\*Corresponding author, Professor, E-mail: wangjt@tsinghua.edu.cn

is always quite small. For example, the sampling time-step is only 1/2048 sec for a controller with a sampling frequency of 2048 Hz. To solve this contradiction, the sub-stepping technique (Bonnet 2006) was proposed and developed. The sub-stepping technique involves splitting tasks which are related to the solution of a numerical substructure into different parts and using different time-steps to execute. The integration time-step of solving the numerical substructure is referred to as the *main time-step*, which is always larger than the sampling time-step of the controller. The signal generation time-step is referred to as the *sub time-step*, which is always identical to the sampling time-step of the controller. The sub-stepping technique was first proposed by Nakashima and Masaoka (1999) to conduct multi-degree-of-freedom (MDOF) RTDHT by dividing numerical substructure analysis into the response analysis task (RAT) and the signal generation task (SGT). Since then, many other researchers emulated it to expand the simulation scale of numerical substructures. Shing *et al.* (2004) proposed a fast hybrid testing system to achieve the real-time response with a high loading rate. A quadratic interpolation method was developed to generate command displacements to ensure the smooth motion of an actuator during iteration of a nonlinear solution. Bonnet *et al.* (2008) used a similar strategy in complex numerical models. The last extrapolated result, used in the new interpolation, was introduced to solve the continuity problem between sub time-steps. Jung *et al.* (2007) presented RTDHT with an implicit time integration scheme, where the sub-stepping technique with a quadratic interpolation was applied to update command displacements during iteration. Chen and Ricles (2008, 2012) applied the sub-stepping technique to MDOF real-time hybrid tests by using a linear ramp generator to smoothly interpolate command displacements in a small time-step.

Only one target computer was used in the aforementioned studies. Reinhorn *et al.* (2004) proposed a RTDHT system with dual target computers. One target computer was used to conduct numerical simulation, and the other was mainly used to perform the cascade control loop to achieve force control as well as compensate time delay. This kind of system was widely applied for the force-based substructuring (Reinhorn *et al.* 2006, Shao *et al.* 2011). Inspired by this unique thought and the sub-stepping technique, Zhu *et al.* (2014) developed another RTDHT system with dual target computers to further improve computation capability of the numerical analysis. As shown in Fig. 1, the RAT was executed in the Target Computer 1 at each main time-step  $\Delta t$ , while the SGT was executed in the Target Computer 2 at each sub time-step  $\delta t$ . A 1240-DOF finite element (FE) numerical substructure was successfully implemented when the main time-step was 40/2048 sec (about 0.02 sec). Comparing with the RTDHT with single target computer, the RTDHT with dual target computers may enhance computing capability of the RAT by executing the SGT independently. Moreover, it also provides a potential for further improving the computing efficiency and accuracy of the RTDHT by assigning more tasks on the second target computer.

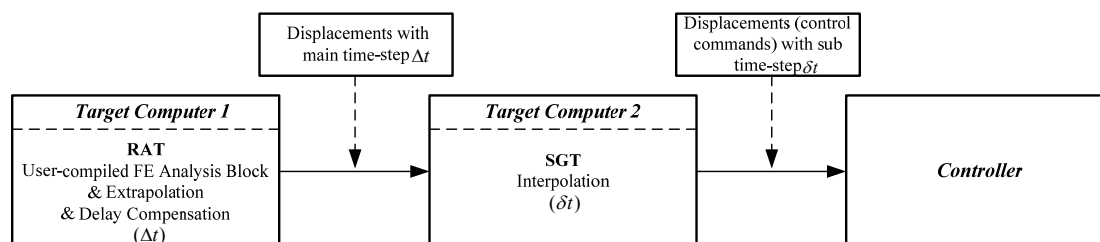


Fig. 1 RAT and SGT processes in the RTDHT system with dual target computers

In addition, the sub-stepping technique results in the incoordination between the real and desired feedback forces. This incoordination is equivalent to introducing an additional time delay of a main time-step  $\Delta t$  into the RTDHT system, which is different from the inherent time delay resulted from the hydraulic serve system. With the main time-step  $\Delta t$  enlarging, the effect of the additional time delay on the RTDHT system becomes remarkable.

To overcome the incoordination between the real and desired feedback forces, an extrapolation procedure is required to predict displacements at the next main time-step in advance. So far, many displacement prediction methods have been proposed to compensate for the time delay. The  $N$ th-order polynomial fitting, a simple and efficient method, has been extensively used in the RTDHT (Nakashima and Masaoka 1999, Horiuchi *et al.* 1999). Nakashima and Masaoka (1999) analyzed the accuracy of 1st to 4th-order polynomial extrapolation and proved that the 3rd and 4th-order polynomials had better accuracy than the other two polynomials when the main time-step is 0.01 sec. Based on the kinematical equations, Horiuchi and Konno (2001) proposed the linear acceleration prediction method which the formulation of Newmark- $\beta$  method was used to predict displacements at the next time-step. Ahmadizadeh *et al.* (2008) proposed a similar prediction method based on the Newmark's explicit method for delay compensation. This Newmark explicit prediction method shows a significant advantage in force measurements during earthquake simulations. Wu *et al.* (2013) analyzed the relationship between the aforementioned prediction methods and the stability of the RTDHT. In addition, Ahmadizadeh *et al.* (2008) also proposed a kind of force correction method to implement delay compensation. The last few displacements and the feedback forces are fitted by two 2nd-order polynomials, respectively. The desired feedback forces are corrected by seeking the time at which the desired displacement occurs.

Above-mentioned displacement prediction methods show good prediction abilities when the main time-step is less than 0.01 sec. However, the main time-step of the numerical substructure may be as much as 0.01 sec to 0.02 sec for some large-scale numerical substructures. This paper focuses on the displacement prediction for delay compensation in the RTDHT with large main time-step. Solutions of existing displacement prediction methods and the force correction method are investigated, and a new prediction scheme based on the explicit integration algorithm is proposed to predict displacement with main time-steps. Numerical simulations indicate that the proposed method has better accuracy in the high frequency range of interest than other prediction methods when the main time-step becomes relatively large. Finally, a series of RTDHTs are conducted to verify the accuracy and effectiveness of the proposed explicit prediction method.

## 2. Incoordination between the real and desired feedback forces

### 2.1 Integration algorithm

#### 2.1.1 Ideal timeline of the integration algorithm

For linear structures, the equations of motion of numerical substructures can be expressed as

$$\mathbf{M}\ddot{\mathbf{u}}_{i+1} + \mathbf{C}\dot{\mathbf{u}}_{i+1} + \mathbf{K}\mathbf{u}_{i+1} = \mathbf{F}_{i+1} + \mathbf{f}_{i+1} \quad (1)$$

where the subscript  $i+1$  denotes the  $(i+1)$ th main time-step,  $\mathbf{u}$ ,  $\dot{\mathbf{u}}$ , and  $\ddot{\mathbf{u}}$  are the displacement, velocity, and acceleration vectors, respectively;  $\mathbf{M}$ ,  $\mathbf{C}$ , and  $\mathbf{K}$  are the mass, damping, and

stiffness matrices, respectively;  $\mathbf{F}$  is the known external force vector; and  $\mathbf{f}=\mathbf{f}(\mathbf{u},\dot{\mathbf{u}},\ddot{\mathbf{u}})$  is the feedback force vector from the physical substructure.

The form of the equation of motion in Eq. (1) is similar to that of the conventional equation in the structure dynamics. The only difference is the existence of the feedback force vector  $\mathbf{f}_{i+1}$ , which depends on  $\mathbf{u}_{i+1}$ ,  $\dot{\mathbf{u}}_{i+1}$ , and  $\ddot{\mathbf{u}}_{i+1}$ .

Assuming that no time delay exists, the ideal timeline at each integration main time-step is schematically illustrated in Fig. 2. At the beginning of  $(i+1)$ th main time-step, the feedback force  $\mathbf{f}_i$  is transmitted from the physical substructure to the target computer for numerical analyzing. Meanwhile, the command displacement  $\mathbf{u}_{i+1}$  is transmitted to the controller for physical loading. During the  $(i+1)$ th main time-step interval, the analysis of the numerical substructure and the loading of the physical substructure are carried out in parallel. At the  $(i+2)$ th main time-step, the same process is implemented.

In the following discussion, we assume that  $\mathbf{u}_i$ ,  $\dot{\mathbf{u}}_i$ ,  $\ddot{\mathbf{u}}_i$ , and  $\mathbf{f}_i$  are known, but  $\mathbf{u}_{i+1}$ ,  $\dot{\mathbf{u}}_{i+1}$ ,  $\ddot{\mathbf{u}}_{i+1}$  are unknown at the beginning of the  $(i+1)$ th main time-step.  $\mathbf{f}_{i+1}$  can be fed back only after  $\mathbf{u}_{i+1}$  is imposed onto the physical substructure. In addition,  $\mathbf{u}_{i+1}$  and  $\dot{\mathbf{u}}_{i+1}$  should be calculated at the beginning of  $(i+1)$ th main time-step, to ensure the desired condition for accurately controlling the loading of the physical substructures. However, for general integration algorithms, only  $\mathbf{u}_{i+1}$  can be calculated at the beginning of  $(i+1)$ th main time-step. If both  $\mathbf{u}_{i+1}$  and  $\dot{\mathbf{u}}_{i+1}$  can be calculated explicitly, this integration algorithm is called the *dual explicit algorithm* in this paper.

### 2.1.2 Dual explicit algorithm

Based on the discrete control theory, Chen and Ricles (2008) proposed the CR algorithm, which is an unconditionally stable, explicit algorithm. RTDHTs conducted by using this algorithm were highly effective (Chen *et al.* 2009). Gui *et al.* (2014) proposed a family of explicit algorithms that contains the CR algorithm as a special case. The general formulation is defined as

$$\mathbf{u}_{i+1} = \mathbf{u}_i + \Delta t \dot{\mathbf{u}}_i + \alpha \Delta t^2 \ddot{\mathbf{u}}_i \tag{2}$$

$$\dot{\mathbf{u}}_{i+1} = \dot{\mathbf{u}}_i + \alpha \Delta t \ddot{\mathbf{u}}_i \tag{3}$$

in which

$$\alpha = 2\lambda(2\lambda\mathbf{M} + \lambda\Delta t\mathbf{C}_0 + 2\Delta t^2\mathbf{K}_0)^{-1}\mathbf{M} \tag{4}$$

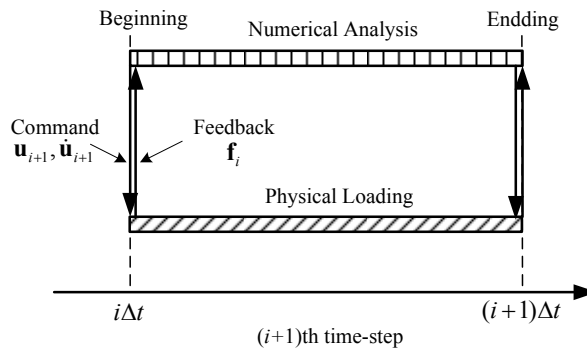


Fig. 2 Ideal timeline at each integration main time-step

where  $\alpha$  is the integration parameter matrix;  $\lambda$  is a parameter that governs the numerical properties; and  $C_0$  and  $K_0$  are the initial damping and stiffness matrices of structure if a nonlinear structure is considered, respectively. Thus  $\alpha$  can be computed before the start of testing and is invariant in the entire integration procedure. For  $\lambda = 4$ , the proposed algorithm is exactly the same as the CR algorithm.

In Eqs. (2) and (3), the displacement and velocity are computed explicitly at each main time-step. Therefore, this family of explicit algorithms belongs to the dual explicit algorithm as defined in Section 2.1.1. This characteristic is potentially attractive in the RTDHT because the loading of the physical substructure can be accurately controlled by both displacement and velocity.

### 2.2 Analysis of the incoordination

This section mainly investigates the incoordination between the real and desired feedback forces when the sub-stepping technique is applied to the RTDHT system.

For the sake of brevity, the ideal timeline presented in Fig. 2 is considered. As schematically shown in Fig. 3,  $\mathbf{u}_{i+1}$  and  $\dot{\mathbf{u}}_{i+1}$  can be calculated using the dual explicit algorithm in Eqs. (2) and (3) at the beginning of the  $(i+1)$ th main time-step with the known  $\mathbf{u}_i$ ,  $\dot{\mathbf{u}}_i$ ,  $\ddot{\mathbf{u}}_i$ , and  $\mathbf{f}_i$ . This process uses little time. Therefore,  $\mathbf{u}_i$  and  $\mathbf{u}_{i+1}$  can be used to generate displacement signals within the time interval of  $\delta t$  (the sub time-step). When these signals are applied to the controller, the feedback forces at the whole  $(i+1)$ th main time-step are measured in sequence with the time interval of  $\delta t$  and  $\mathbf{f}_{i+1}$  will be sent to the Target Computer 1 at the end of the  $(i+1)$ th main time-step. In this case,  $\ddot{\mathbf{u}}_{i+1}$  cannot be calculated at the beginning of the  $(i+1)$ th main time-step because it depends on  $\mathbf{f}_{i+1}$ . This condition means that  $\mathbf{f}_{i+1}$  is the desired feedback force at the beginning of the  $(i+1)$ th main time-step. However, only  $\mathbf{f}_i$  is the available feedback force.

Therefore, the incoordination between the real and desired feedback forces is inevitable. This incoordination is equivalent to introducing an additional time delay of one main time-step into the RTDHT system, which may cause instability. Hence, the extrapolation procedure or other similar methods should be considered to predict displacement after obtaining the  $\mathbf{u}_{i+1}$ .

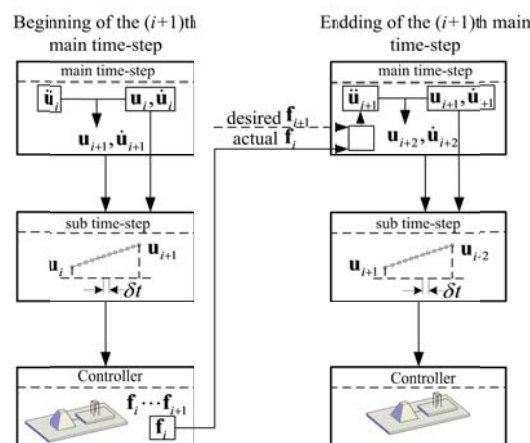


Fig. 3 Explanation of incoordination between the desired and real feedback forces



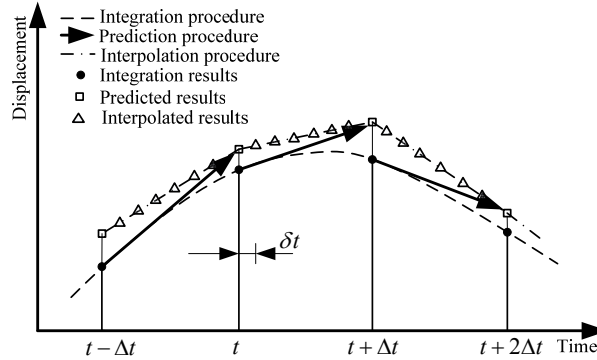


Fig. 5 Time-step switch strategy in the RTDHT system with dual target computers

For the RTDHT system with dual target computers, another strategy is used in this paper to solve the aforementioned sudden jump problem. As shown in Fig. 5, at time  $t$ , the displacement after the time interval of  $\Delta t$  is predicted in the Target Computer 1 in advance, and then the Target Computer 2 generates displacement signals by using the linear interpolation synchronously. Because all displacement signals are generated by interpolation, the switch from extrapolation to interpolation during one main time-step is unnecessary. It guarantees the smooth movement of loading equipments.

### 3. Delay compensation solutions for large time-step

As stated in the Section 1, some prediction methods which contain force and displacement predictions have been widely used for delay compensation. Those well-developed prediction methods exhibit good prediction abilities when the main time-step is less than 0.01 sec. This section firstly proposes a new displacement prediction method based on the dual explicit algorithm. Then the accuracy comparison between the proposed and the known prediction methods applied for large main time-step is analyzed theoretically and numerically in detail.

#### 3.1 Dual explicit prediction method

This section proposes a new displacement prediction method (called the *dual explicit prediction method* in this paper) based on the dual explicit algorithm by using the displacement  $\mathbf{u}_{i+1}$  and the velocity  $\dot{\mathbf{u}}_{i+1}$  explicitly calculated at the  $(i+1)$ th main time-step. The displacement prediction is shown conceptually in Fig. 6. The following 4th-order polynomial is employed to predict the acceleration

$$\ddot{\mathbf{u}}_{i+1}^p = \sum_{k=i-4}^i a_{k+1} \ddot{\mathbf{u}}_k \tag{5}$$

where  $\ddot{\mathbf{u}}_{i+1}^p$  is the predicted acceleration, and  $a_{k+1}$  is the polynomial coefficient. Thus, the  $n$ th predicted displacement can be calculated by using the displacement formulation in the dual explicit algorithm and is given by

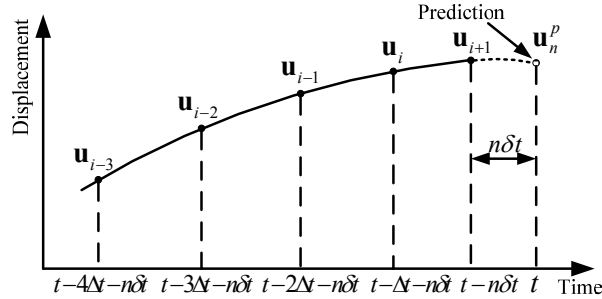


Fig. 6 Displacement prediction

$$\mathbf{u}_n^p = \mathbf{u}_{i+1} + n\delta t \dot{\mathbf{u}}_{i+1} + \alpha_1 (n\delta t)^2 \ddot{\mathbf{u}}_{i+1} \tag{6}$$

where  $\mathbf{u}_n^p$  is the predicted displacement. Compared with Eq. (2), the prediction error is caused solely by the predicted  $\ddot{\mathbf{u}}_{i+1}^p$ . Compared with the Newmark’s explicit prediction method, this method reduces the predicted time interval from  $\Delta t + n\delta t$  to  $n\delta t$ .

### 3.2 Accuracy analysis

The accuracy of displacement prediction methods can be evaluated by considering the vibrating response of the structures under a sinusoidal excitation (Nakashima and Masaoka 1999). Given that a SDOF structure vibrates sinusoidally with the amplitude  $A$  and the circle frequency  $\omega$ ,

$$u = A \sin \omega t \tag{7}$$

where  $u$  is the exact displacement, and  $\omega = 2\pi f$  with  $f$  as the excited frequency. The displacement, velocity, and acceleration of previous main time-steps are given by the following equation and its derivatives:

$$u_{i+1-m} = A \sin \omega(t - m\Delta t - n\delta t) \tag{8}$$

where  $m$  is the number of previous main time-steps. Then, the predicted displacement  $u_n^p$  can be obtained by inserting Eq. (8) and its derivatives into the corresponding formulations of displacement prediction methods. The unified equation of the predicted displacement with the predicted time interval  $n\delta t$  can be expressed as follows

$$u_n^p = A\beta \sin(\omega t + \phi_n) \tag{9}$$

with

$$\begin{cases} \beta = \sqrt{C_n^2 + S_n^2} \\ \phi_n = \arctan \frac{S_n}{C_n} \end{cases} \tag{10}$$

and

$$\begin{cases} C_n = \sum_{k=0}^m a_{i+1-k} \cos \omega(k\Delta t + n\delta t) \\ S_n = -\sum_{k=0}^m a_{i+1-k} \sin \omega(k\Delta t + n\delta t) \end{cases} \quad (11)$$

where  $\beta$  is the amplitude change; and  $\phi_n$  is the phase shift.  $C_n$  and  $S_n$  are only related to  $\omega$  when both  $n\delta t$  and  $\Delta t$  are constant. Eqs. (9)-(11) indicate that the amplitude change and the phase shift can be regarded as indexes of the error between the target and predicted displacements. The precise solution, i.e., without any error, is defined as the amplitude magnification of 1 and the phase shift of 0.

The prediction methods in this study aim to predict the displacement  $u_{i+2}^p$ , e.g.,  $u_n^p = u_{i+2}^p$ . The amplitude change and phase shift with  $\omega\Delta t$  are plotted in Fig. 7 for different prediction methods (2nd to 4th-order polynomial method, the linear acceleration prediction method, the Newmark's explicit prediction method and the proposed dual explicit prediction method). For the dual explicit prediction method, the value of  $\lambda$  depends on that used in dual explicit algorithm for numerical substructure analysis. For comparing the effect of the parameter  $\lambda$  on the accuracy of the scheme, three cases are conducted with  $\lambda = 11.5, 4$  and  $3$ , respectively. According to Gui *et al.* (2013), the algorithm has the best computing accuracy when  $\lambda = 11.5$ , and is unconditionally stable when  $\lambda = 4$  and  $3$ .

When  $\omega\Delta t < 0.3$ , both amplitude change and phase shift display negligible dispersion for all prediction methods; however, their changing trends are different with the increase of  $\omega\Delta t$ . In Fig. 7(a), it is evident that the dual explicit prediction methods with  $\lambda = 11.5, 4$  and  $3$  have a small dispersion in the range of  $0.3 < \omega\Delta t < 1.4$ , especially in  $1.0 < \omega\Delta t < 1.4$  (corresponding to the frequency range of 8-11.4 Hz when  $\Delta t = 40/2048$  sec), compared with other prediction methods. It demonstrates that the dual explicit prediction method has better accuracy than other considered methods.

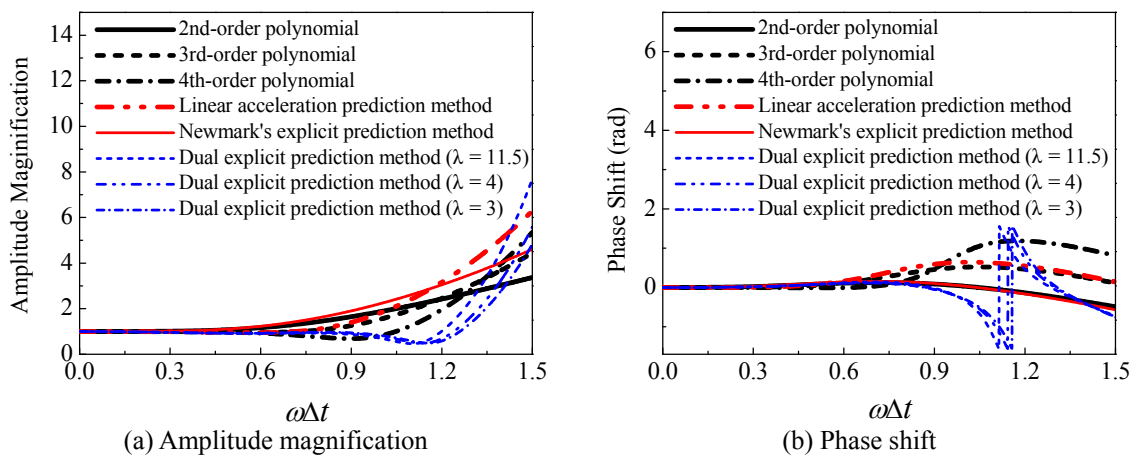


Fig. 7 Errors generated by various displacement prediction methods

For the phase shift in Fig. 7(b), it is clear that the phase shift of the dual explicit prediction method approaches to zero in a wide range of  $0 < \omega\Delta t < 0.9$ . However, a sudden change occurs for the dual explicit prediction methods with  $\lambda = 11.5, 4$  and  $3$  when  $\omega\Delta t$  approaches to  $1.1$  and the corresponding phase shift is equal to  $\pm\pi/2$ . This sudden change, called the jump discontinuity (belonging to the discontinuity point of the first kind) in mathematics, is a common phenomenon since the formulation of the phase shift  $\phi_n$  is the arctangent function as shown in Eq. (10). Other prediction methods in Fig. 7 will lead to similar sudden change when the phase shift approaches to  $\pm\pi/2$  with the increase of  $\omega\Delta t$ .

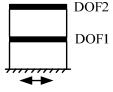
In conclusion, the proposed dual explicit prediction method shows good prediction accuracy when the main time-step  $\Delta t$  enlarges to  $40/2048$  sec, especially in high-range of frequency (8.1-11.4 Hz). Since the concerned earthquake wave frequency is about 0-10 Hz in structural dynamics, this proposed scheme is suitable for RTDHT to obtain accurate high frequency displacement response when a relative large predicted time interval appears.

### 3.3 Numerical validation test

A numerical example of a 2-DOF structure is performed to verify the accuracy levels achieved by using the Newmark's explicit prediction method, the 3rd-order polynomial, and the proposed dual explicit prediction method. The properties of the structure are listed in Table 1. The damping matrix for the structure is based on the Rayleigh proportional damping with 5% damping ratio for both modes. The external acceleration input is a sinusoidal sweep wave with the constant amplitude of 0.15 g and varying frequency from 0 Hz to 10 Hz. The target displacements of DOF1 are calculated by the dual explicit algorithm with  $\lambda = 3$ . Meanwhile, the predicted displacements of the DOF1 are determined by using the three prediction methods on the basis of the target displacements, respectively. The predicted time interval is equal to the main time-step  $\Delta t$ . Figs. 8 and 9 present the time history and Fourier spectrum of the target and predicted displacements with  $\Delta t = 20/2048$  sec and  $\Delta t = 40/2048$  sec, respectively.

When  $\Delta t = 20/2048$  sec, the results of the 3rd-order polynomial and the dual explicit prediction method agree quite well with the target displacement in the time domain, as shown in Fig. 8(a). But the results of the Newmark's explicit prediction method are slightly larger than the target displacement. In the frequency domain as shown in Fig. 8(b), the displacements predicted by the 3rd-order polynomial and the dual explicit prediction method match well with the target displacements; however, the Newmark's explicit prediction method slightly overestimates the displacements response at the resonant frequencies, which indicates the same scenario as observed in time domain.

Table 1 Structural properties of the numerical model

Model	Mass (kg)	Stiffness (N/m)	Damping(N·sec/m)	Natural Frequency (Hz)
	$\begin{bmatrix} 1000 & 0 \\ 0 & 1000 \end{bmatrix}$	$\begin{bmatrix} 2 \times 10^6 & -10^6 \\ -10^6 & 10^6 \end{bmatrix}$	$\begin{bmatrix} 4251.954 & -1422 \\ -1422 & 2829.954 \end{bmatrix}$	$\begin{bmatrix} 3.1 \\ 8.1 \end{bmatrix}$

When  $\Delta t = 40/2048$  sec, the discrepancy of the Newmark's explicit prediction method becomes more striking in both the time and frequency domains (Fig. 9). The amplitude amplification occurs in a large range of frequency. The 3rd-order polynomial also obtains the amplified amplitude in the frequency range of 8-10 Hz. In contrast, the prediction displacement achieved by the dual explicit prediction method still agrees well with the target displacement.

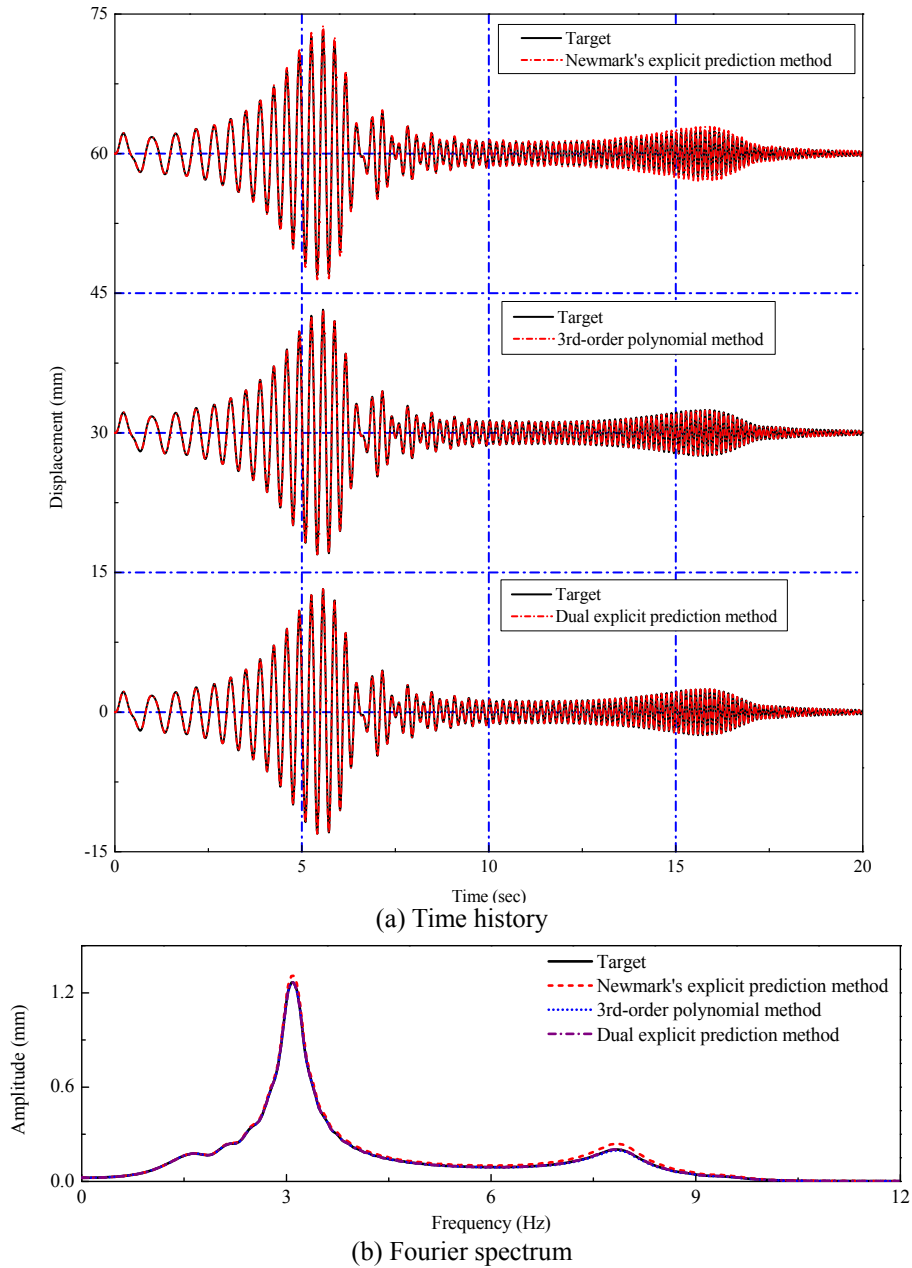


Fig. 8 Target and predicted displacement responses of DOF1 for a 2-DOF structure ( $\Delta t = 20/2048$  sec)

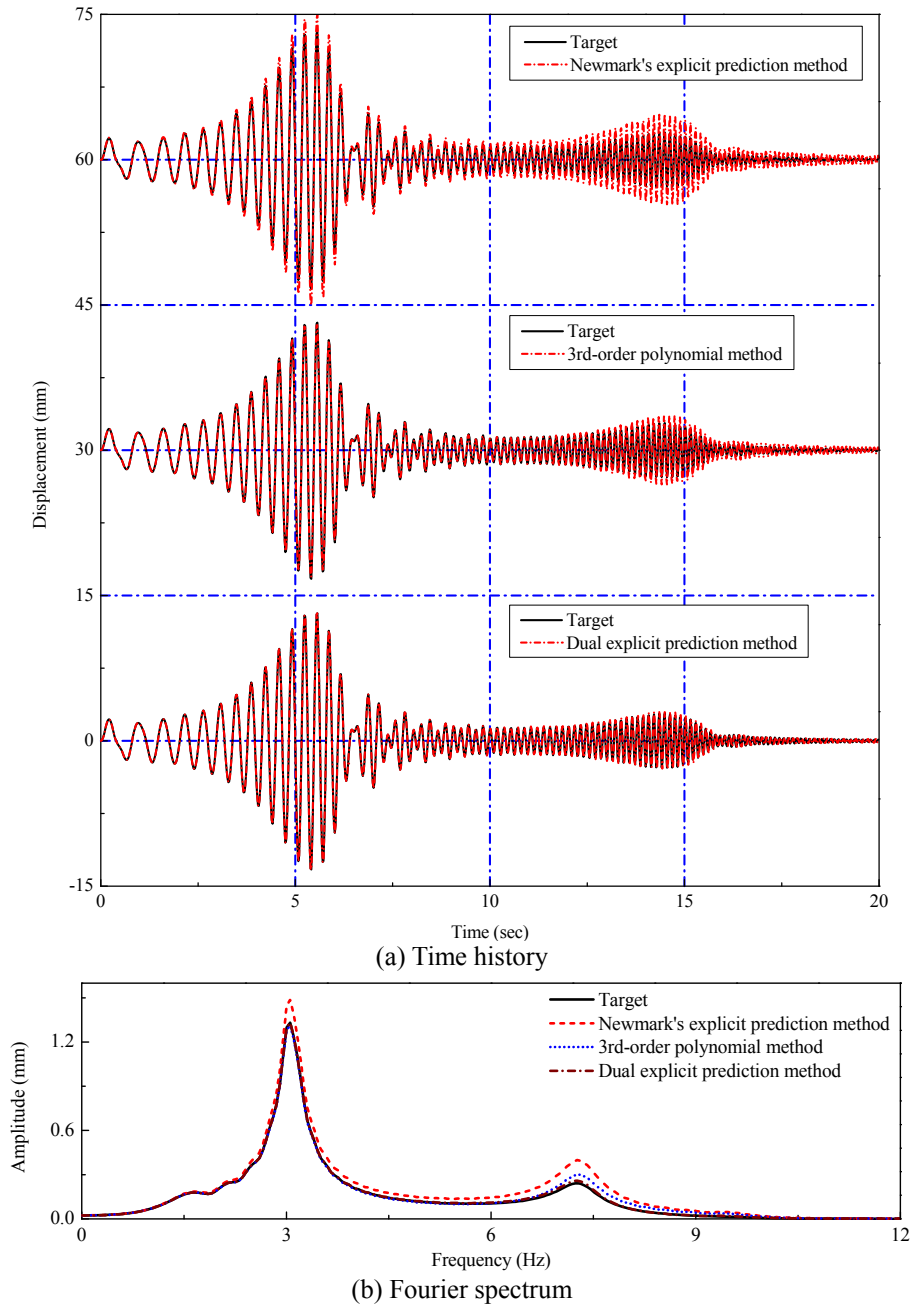


Fig. 9 Target and predicted displacement responses of DOF1 for a 2-DOF structure ( $\Delta t = 40/2048$  sec)

Table 2 Normalized root mean square errors (%) of different prediction methods

Prediction method	$\Delta t = 20/2048$ sec	$\Delta t = 40/2048$ sec
Newmark's explicit prediction method	6.74	29.05
3rd-order polynomial	1.03	16.33
dual explicit prediction method	1.43	9.44

To quantitatively evaluate the performance of the prediction methods, the normalized root mean square (NRMS) error (Chae *et al.* 2013) between the target and predicted displacements is further calculated as follows

$$NRMS \text{ error} = \sqrt{\frac{\sum_{i=1}^N (u_i^t - u_i^p)^2}{\sum_{i=1}^N (u_i^t)^2}} \quad (12)$$

where  $u_i^t$  and  $u_i^p$  are the target and predicted displacement at  $i$ th main time-step, respectively. The NRMS errors for those three prediction methods are summarized in Table 2.

It can be seen from Table 2 that the NRMS errors of the 3rd-order polynomial and the dual explicit prediction method are smaller than those of the Newmark's explicit prediction method when  $\Delta t = 20/2048$  sec; and the NRMS error of the dual explicit prediction method is smaller than those of the 3rd-order polynomial and the Newmark's explicit prediction method when  $\Delta t = 40/2048$  sec.

## 4. Experimental analysis

### 4.1 The RTDHT system with dual target computers

The RTDHT system with dual target computers for simulating large-scale numerical substructures is shown in Fig. 10. The system comprises three components: the distributed real-time calculation system, the shaking table loading system, and the data acquisition and transmission system (Wang *et al.* 2011, Zhu *et al.* 2014). The xPC-Target toolbox (MATLAB, 2006) is employed as the solution in the distributed real-time calculation system. The shaking table loading system consists of the MTS 469D digital controller, two shaking tables, and oil source. The data acquisition and transmission system uses PXI and LabVIEW to construct the data acquisition platform. SCRAMNet cards are also used to ensure real-time data transmission.

There are two identical uni-axial shaking tables, manufactured by MTS Company. Each table has a 1.5 m  $\times$  1.5 m working area and a bearing capacity of 2 ton. The maximum acceleration can reach up to 3.6 g when the table is bare and 1.2 g when the table loads to its full capacity. The excited frequency range is 0–50 Hz. The Three Variable (displacement, velocity and acceleration) Control is used for the tables. MATLAB/Simulink is integrated into the 469D digital controller platform to achieve real-time hybrid control capabilities. Consequently, all controller feedback outputs are made available in Simulink, while commands or controller correction signals generated by Simulink can drive the controller command inputs.

#### 4.2 Experimental setup

The tested structure is a three-storey shear frame mounted on a semi-infinite elastic foundation. The entire structure and its substructure splitting are shown in Fig. 11. The superstructure is physically tested by the shaking table and the elastic foundation is numerically simulated by the finite element method.

The semi-infinite elastic foundation is idealized as a finite-sized region with fixed boundaries and simulated with an FE model as shown in Fig. 11(b). The model measures  $60\text{ m} \times 40\text{ m}$  and consists of 96 four-node quadrilateral elements with 117 nodes. A total of 234 DOFs are included in the model. The material properties of the foundation are as follows: mass density of  $2000\text{ kg/m}^3$ ; Poisson's ratio of 0.2; and elastic modulus of  $4000\text{ MPa}$ . The selected mass and the acceleration similitude ratios for the superstructure are  $c_m = 2 \times 10^3$  and  $c_a = 1$ , respectively. Other similitude ratios can be deduced based on the similitude relation (Wang *et al.* 2011).

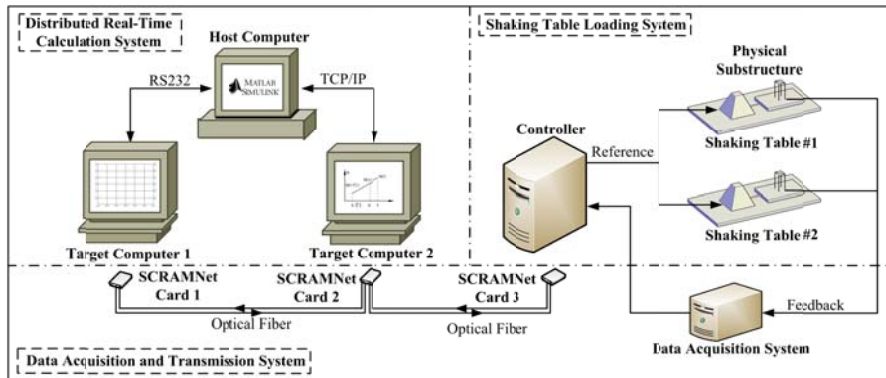


Fig. 10 Outline of the RTDHT system with dual target computers

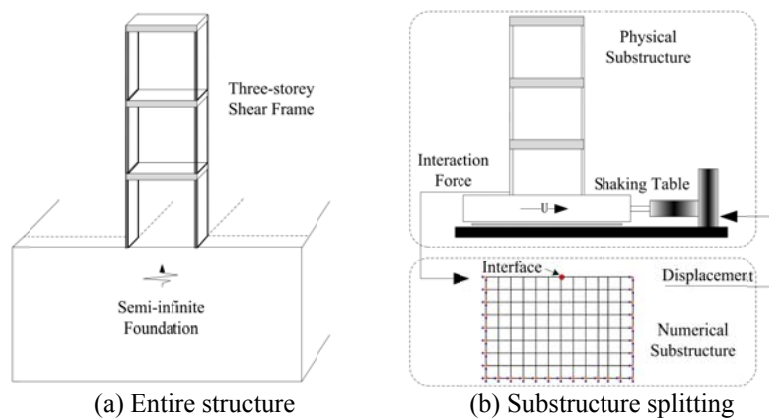


Fig. 11 Substructure splitting of the three-storey shear frame mounted on the semi-infinite foundation

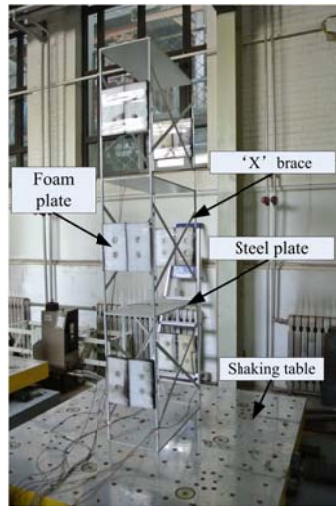


Fig. 12 Photograph of the three-storey shear frame

Fig. 12 shows the physical substructure of the three-storey shear frame. Each storey is 0.69 m high, and has four welded thin supporting legs and a steel plate on its top. Each steel plate has a  $0.61 \text{ m} \times 0.3 \text{ m}$  area and a mass of 14.274 kg. Since the shaking table only can load unidirectional, two “X” braces are welded in each storey perpendicular to the direction of excitation to increase the lateral stiffness. Two plastic foam plates are added in each storey paralleled to the direction of excitation to introduce damping for the entire shear frame. The first three-order natural frequencies of the frame measured by white noise sweeping are 2.6, 8.1, and 12.6 Hz, respectively. The shear force between the numerical and physical substructures is measured by strain gauges based on the principle of Wheatstone bridges (Wang *et al.* 2011).

#### 4.3 Experimental results

The dual explicit algorithm with  $\lambda = 3$  is applied to analyze the numerical substructure, thereby ensuring unconditionally stable solutions. Five RTDHTs are considered. Among them, four RTDHTs are conducted using the four prediction methods (the proposed dual explicit prediction method, the 3rd-order polynomial, the Newmark’s explicit prediction method and the force correction method, respectively) with the same time parameters: the main time-step  $\Delta t = 40/2048$  sec in the Target Computer 1, and the sub time-step  $\delta t = 1/2048$  sec in the Target Computer 2 (identical to the sampling time-step of the MTS controller). So the additional time delay compensated by these four prediction methods is equal to  $\Delta t$ . The remaining one is conducted as a reference RTDHT to obtain the “exact” results, where both the main time-step  $\Delta t$  and the sub time-step  $\delta t$  are all selected as  $1/2048$  sec. In the reference RTDHT, the incoordination problem disappears and in turn the compensation for the additional time delay is unnecessary.

In all the above-mentioned five RTDHTs, the inherent time delay of the hydraulic servo system is calibrated to around 0.01 sec. It is compensated by using the commonly-used compensation method developed by Wallace *et al.* (2005).

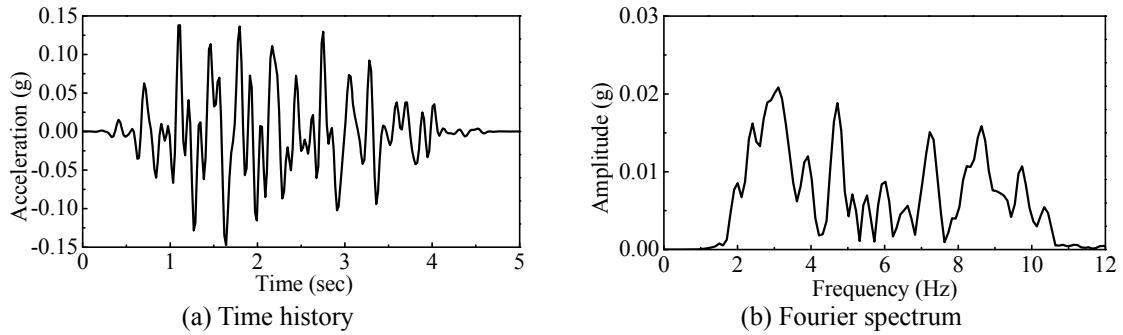


Fig. 13 Time history and the Fourier spectrum of the artificial seismic wave

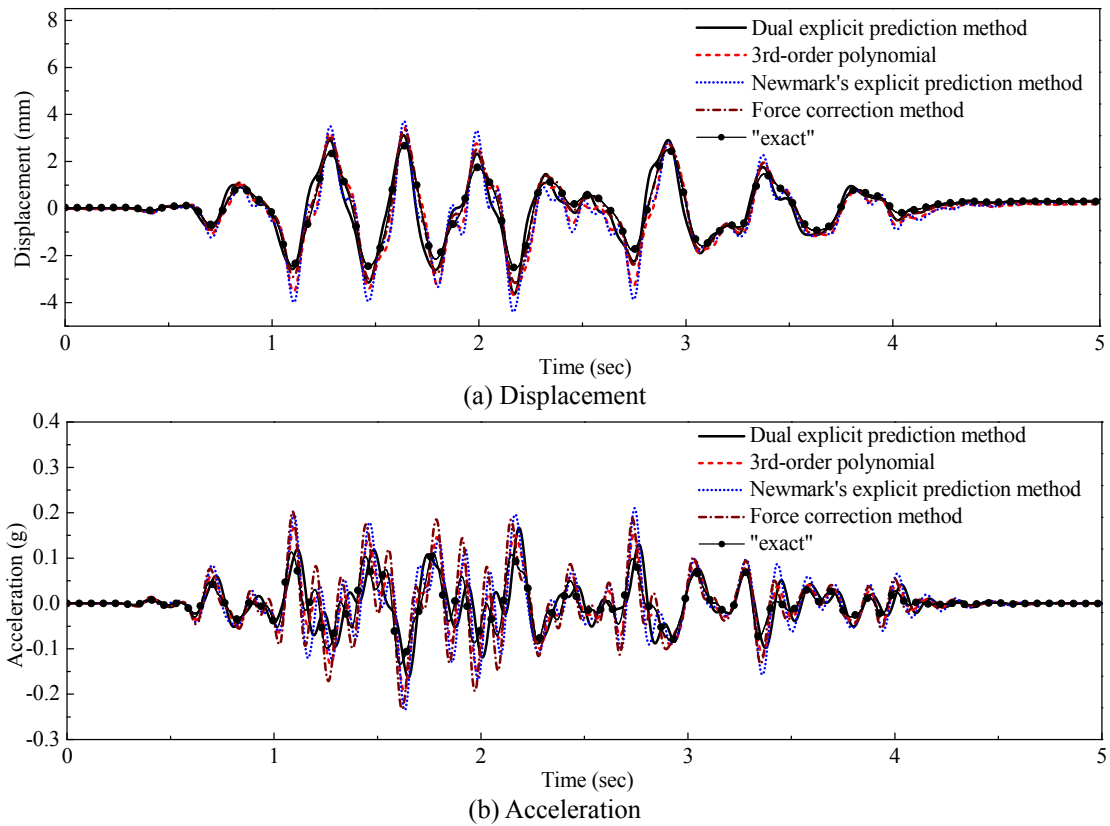


Fig. 14 Displacement and acceleration histories at the bottom of the three-storey shear frame

The artificial seismic wave is applied as the free-field input to excite the structure. The interface between the numerical and physical substructures is the input point, as shown in Fig. 11(b). The peak acceleration is 0.15 g. Fig. 13 depicts the time history and Fourier spectrum of the artificial wave.

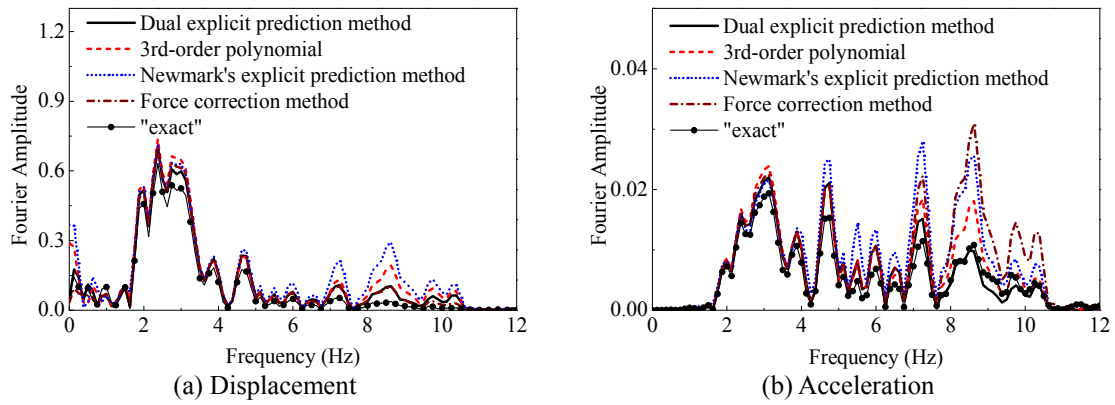


Fig. 15 Fourier spectrum of displacement and acceleration at the bottom of the three-storey shear frame

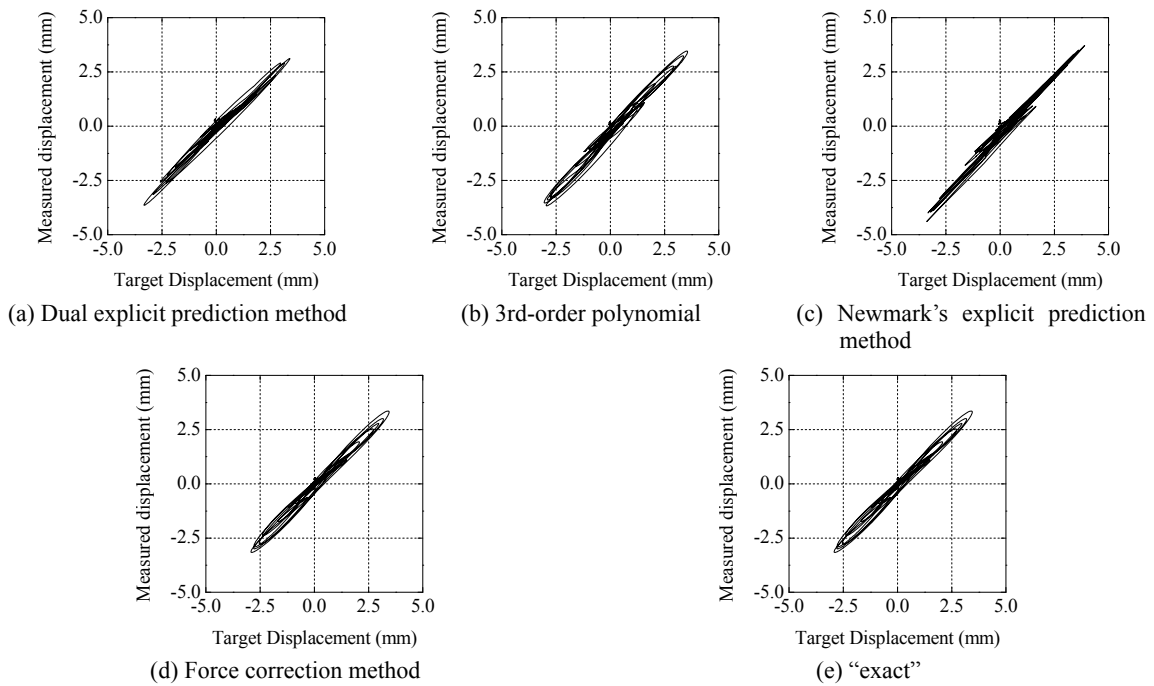


Fig. 16 Synchronization subspace plots of the target and measured displacement at the bottom of the three-storey shear frame

Fig. 14 presents the dynamic displacement and the acceleration responses at the bottom of the three-storey shear frame (the interface of the numerical and physical substructures). As shown in Fig. 14(a), the peak displacement of the “exact” result is 2.73 mm, and those obtained by using the dual explicit prediction method, the 3rd-order polynomial method, Newmark’s explicit prediction method, and the force correction method are determined as 3.10, 3.47, 3.76, and 3.36 mm, with errors of 13.55%, 27.11%, 37.73%, and 23.08%, respectively. In Fig. 14(b), the acceleration obtained by using the dual explicit prediction method is the closest to the “exact” result. A similar trend is demonstrated by the Fourier spectrum shown in Fig. 15. Fig. 16 shows the synchronization subspace plots for these five RTDHTs. The deviations from the diagonal straight line in all plots are very small, which indicates the good performance of the compensation methods used during testing.

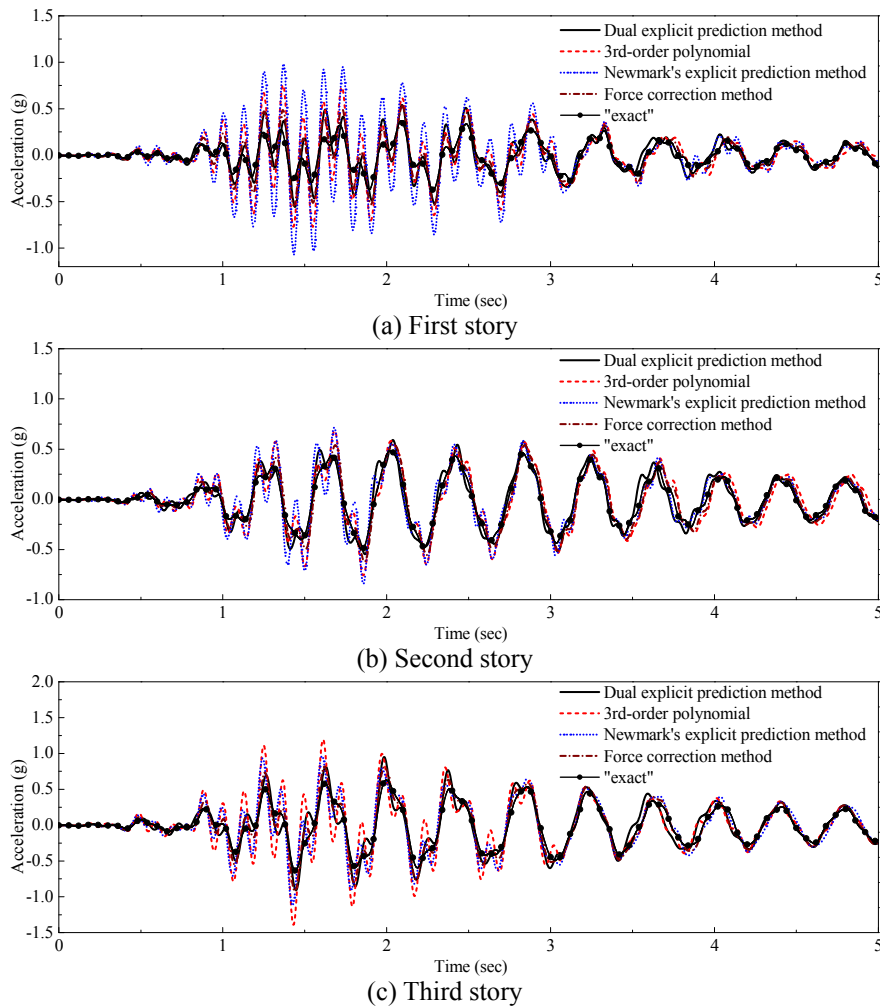


Fig. 17 Acceleration histories of the three-storey shear frame

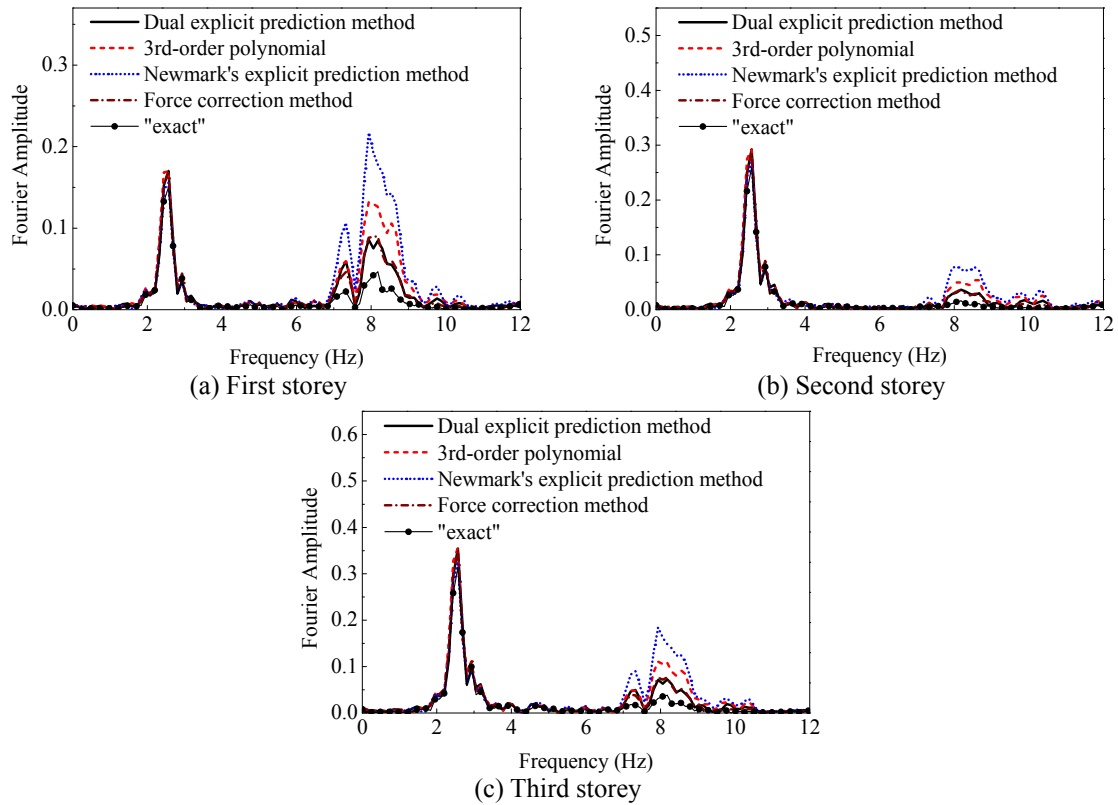


Fig. 18 Fourier spectrum of the accelerations of the three-storey shear frame

Figs. 17 and 18 present the acceleration responses of the three stories of the frame. Similar conclusions can be drawn from the results in the time and frequency domains. The dual explicit prediction method yields the highest prediction efficiency. The Newmark’s explicit prediction method shows the most significant error because of the predicted time interval which is as large as two times of the main time-step.

In summary, compared with other displacement prediction methods and the force correction method, the proposed dual explicit prediction method exhibits the highest prediction accuracy, especially in the high frequency range.

### 5. Conclusions

This study focuses on the RTDHT system with dual target computers to simulate large-scale numerical substructures by using the sub-stepping technique. Given that a large main time-step is used to fully extend the simulation scale of the numerical substructure, the incoordination between the real and desired feedback force which is equivalent to introducing an additional time delay in systems must be considered. Hence, displacement prediction or feedback force correction is important for delay compensation. To address this problem, a new dual explicit displacement

prediction method based on the explicit integration algorithm is proposed.

The proposed method is compared with the other three existing displacement prediction methods, namely, the  $N$ th-order polynomial prediction method, the linear acceleration prediction method, and the Newmark's explicit prediction method. Theoretical and numerical analysis show that the proposed dual explicit prediction method exhibits higher accuracy than other methods in the high frequency range. This finding is indicated by a relatively large predicted time interval. Finally, RTDHTs of a three-storey shear frame mounted on a semi-infinite foundation are successfully implemented with the force correction method, the 3rd-order polynomial method, the Newmark's explicit prediction method, and the proposed method. The proposed dual explicit prediction method demonstrates the highest reduction in high-frequency response error which demonstrates its good ability for displacement prediction with large time-step.

Considering that the performance of a delay compensation method should be assessed by accuracy as well as stability, the stability analysis of the proposed method for compensating relatively large time delay is also crucial. This application will be discussed in future studies.

## Acknowledgements

This work is financially supported by the National Natural Science Foundation of China (Nos. 51179093, 91215301 and 41274106) and the Specialized Research Fund for the Doctoral Program of Higher Education (No. 20130002110032).

## References

- Ahmadizadeh, M., Mosqueda, G. and Reinhorn, A.M. (2008), "Compensation of actuator delay and dynamics for real-time hybrid structural simulation", *Earthq. Eng. Struct. D.*, **37**(1), 21-42.
- Bonnet, P.A. (2006), The development of multi-axis real-time substructure testing, Ph.D. Dissertation, University of Oxford, Oxford.
- Bonnet, P.A., Lim, C.N., Williams, M.S., Blakeborough, A., Neild, S.A., Stoten, D.P. and Taylor, C.A. (2007), "Real-time hybrid experiments with Newmark integration, MCSmd outer-loop control and multi-tasking strategies", *Earthq. Eng. Struct. D.*, **36** (1), 119-141.
- Bonnet, P.A., Williams, M.S. and Blakeborough, A. (2008), "Evaluation of numerical time-integration schemes for real-time hybrid testing", *Earthq. Eng. Struct. D.*, **37**(13), 1467-1490.
- Chen, C. and Ricles, J.M. (2008), "Development of direct integration algorithms for structural dynamics using discrete control theory", *J. Eng. Mech.-ASCE.*, **134** (8), 676-683.
- Chen, C. and Ricles, J.M. (2012), "Large-scale real-time hybrid simulation involving multiple experimental substructures and adaptive actuator delay compensation", *Earthq. Eng. Struct. D.*, **41** (3), 549-569.
- Chen, C., Ricles, J.M., Marullo, T.M. and Mercan, O. (2009), "Real-time hybrid testing using the unconditionally stable explicit CR integration algorithm", *Earthq. Eng. Struct. D.*, **38** (1), 23-44.
- Gui, Y., Wang, J.T., Jin, F., Chen, C. and Zhou, M.X. (2014), "Development of a family of explicit algorithms for structural dynamics with unconditional stability", *Nonlinear Dyn.*, **77**(4), 1157-1170.
- Horiuchi, T., Inoue, M., Konno, T. and Namita, Y. (1999), "Real-time hybrid experimental system with actuator delay compensation and its application to a piping system with energy absorber", *Earthq. Eng. Struct. D.*, **28** (10), 1121-1141.
- Horiuchi, T., and Konno, T. (2001), "A new method for compensating actuator delay in real-time hybrid experiments", *Philos. T. R. Soc. London. A*, **359**(1786), 1893-1909.
- Jung, R.Y., Benson Shing, P., Stauffer, E. and Thoen, B. (2007), "Performance of a real-time pseudodynamic

- test system considering nonlinear structural response”, *Earthq. Eng. Struct. D.*, **36** (12), 1785-1809.
- MATLAB. (2006), The MathWorks, Inc., Natick, Mass.
- Nakashima, M. and Masaoka, N. (1999), “Real-time on-line test for MDOF systems”, *Earthq. Eng. Struct. D.*, **28** (4), 393-420.
- Reinhorn, A.M., Sivaselvan, M.V., Liang, Z. and Shao, X.Y. (2004), “Real-time dynamic hybrid testing of structural systems”, *Proceedings of 13th World Conference on Earthquake Engineering*, Vancouver, Canada, Paper No. 1644.
- Reinhorn, A.M., Shao X.Y., Sivaselvan, M.V., Pitman, M. and Weinreber, S. (2006), “Real time dynamic hybrid testing using shake tables and force-based substructuring”, *Proceedings of the ASCE 2006 Structures Congress*, St. Louis, Missouri, USA, May.
- Schellenberg, A., Mahin, S.A. and Fenves, G.L. (2009), *Advanced implementation of hybrid simulation, PEER Report 2009/104*.
- Shao, X., Reinhorn, A.M. and Sivaselvan, M.V. (2011), “Real-time hybrid Simulation using shake tables and dynamic actuators”, *J. Struct. Eng. - ASCE*, **137**(7), 748-760.
- Shing, P., Wei, Z., Jung, R.Y. and Stauffer, E. (2004), “NEES FAST HYBRID TEST SYSTEM AT THE UNIVERSITY OF COLORADO”, *Proceeding of 13th World Conference on Earthquake Engineering*, Vancouver, Canada, August.
- Wallace, M.I., Wagg, D.J. and Neild, S.A. (2005), “An adaptive polynomial based forward prediction algorithm for multi-actuator real-time dynamic substructuring”, *Proc. R. Soc. A*, **461** (2064), 3807-3826.
- Wu, B., Wang, Z. and Bursi O.S. (2013), “Actuator dynamics compensation based on upper bound delay for real-time hybrid simulation”, *Earthq. Eng. Struct. D.*, **42**(12), 1749-1795.
- Wang, Q., Wang, J.T., Jin, F., Chi, F.D. and Zhang, C.H. (2011), “Real-time dynamic hybrid testing for soil-structure interaction analysis”, *Soil Dyn. Earthq. Eng.*, **31**(12), 1690-1702.
- Zhu, F., Wang, J.T., Jin, F., Zhou, M.X. and Gui, Y. (2014), “Simulation of large-scale numerical substructure in real-time dynamic hybrid testing”, *Earthq. Eng. Eng. Vib.*, **13**(4), 599-609.